Institute of Industrial Engineering

College of Engineering

National Taiwan University

Linear Algebra and Its Applications in
Three-dimensional Geometric Morphometrics

Li-Wei Yang

Advisor: Argon Chen Ph.D.

December, 2022

Abstract

In this study, linear algebra methods used in Geometric Morphometrics are explained, and a practical example in paleontology is set forth. This research supports a recent study in morphology between Felinae and Machairodontinae. Despite the scarcity of fossil records of early machairodontines, the recent study still retrieved *Promegantereon ogygia* and *Machairodus aphanistus* from Batallones localities in the Madrid region. This study verifies the result of that recent study and provides different visualization of the morphology.

Keywords: Geometric Morphometrics, Linear Algebra, Generalized Procrustes Analysis, Principal Component Analysis

Contents

List of Figures

List of Tables

Chapter 1   Rationale

I conducted a robotic research project using the morphing methods in SlicerMorph [1], an extension focused on 3D morphology in 3D Slicer [2, 3] software. At that time, I had little knowledge of linear algebra. When I encountered those linear algebra methods in SlicerMorph, including Similarity Transform, Generalized Procrustes Analysis, Principal Component Analysis, etc., I could not understand how they worked. This semester, I had the pleasure of auditing this course, and I would like to end this course from where I began my linear algebra journey. SlicerMorph is for a domain I am unfamiliar with－3D Geometric Morphometrics. Conducting a research project on a domain I am not familiar with is challenging yet exciting. To finish the project on time, this term project is based on a recent study. I will explain their work and mine from a linear algebra perspective.

Chapter 2   Problem Background

2.1   3D Geometric Morphometrics (3D GM)

Morphometrics is a study that compares the shape of organisms or organs and tries to find the shape's covariance with other variables [4]. "*Defined as the fusion of geometry and biology, morphometrics deals with the study of form in two- or three-dimensional space*" [5]. Traditional morphometrics relies on measurements, typically measuring the lengths, widths, masses, angles, ratios, and areas of organisms. The drawback of measurements is that they are highly correlated, and they contain little information about the spatial distribution of shape changes across the organism [6]. In contrast to traditional morphometrics, 3D geometric morphometrics (3D GM) preserves spatial information using landmarks, a set of points that have anatomical meanings and are present among all samples. There are three types of landmarks:

Type I: the landmark point is placed closest to the target structure.

Type II: the landmark point is placed in the tip, local minima or maxima of curvature in the target structure.

Type III: the landmark point is placed farthest from the target structure.

In addition, there are also semilandmarks that are placed evenly on the curves to provide more information about the shape [7]. These semilandmarks are often confined at the two ends to model a curve structure.

2.2   Felinae and Machairodontinae

In the previous study [8], two types of machairodontines from the late Miocene, *Promegantereon ogygia* and *Machairodus aphanistus* were considered not contemporaneous, and a morphological drift between cavities was described for these two species. A more recent study [9] rejects this hypothesis. In this work, we try to analyze the morphology of these two species along with other felines and machairodontines to validate the argument proposed by the recent study.

Chapter 3   Linear Algebra Solutions

3.1   Orientation Matching

Before conducting 3D Geometric Morphometrics, the best practice is first to register all the samples using landmarks. The fiducial registration module in 3D Slicer [2, 3] can help us register landmarks. The module implements Similarity Transform, which point-wisely matches landmarks by translation, rotation, and scaling.

3.2   Orthogonal Procrustes Problem

After all the landmarks are registered, we could analyze the shapes by conducting a Generalized Procrustes Analysis (GPA). GPA is, in essence, solving the Orthogonal Procrustes Problem for a mean shape. The Orthogonal Procrustes Problem is a matrix approximation problem. Given two matrices A and B, one is asked to find an orthogonal matrix Ω which most closely maps A to B [10, 11].

$$R = \arg\min_{\Omega} \|\Omega A - B\|_F \quad \text{subject to} \quad \Omega^T \Omega = I \tag{3.1}$$

Where $\| * \|_F$ is the Frobenius norm of a matrix.

The solution to this problem is proposed by [12], "*This problem is equivalent to finding the nearest orthogonal matrix to a given matrix $M = BA^T$, i.e. solving the closest orthogonal approximation problem.*

$$\min_R \|R - M\|_F \quad \text{subject to} \quad R^T R = I \tag{3.2}$$

To find matrix R, one uses the singular value decomposition (for which the entries of Σ are non-negative): $M = U\Sigma V^T$ to write $R = UV^T$." [11]

3.3 Generalized Procrustes Analysis

In the below section, notations are identical to [13] for the sake of clarity.

Generalized Procrustes analysis is like solving the Orthogonal Procrustes Problem, but the target matrix becomes the mean shape of all the landmarks instead of a sample. Assuming we have a set of landmarks $\boldsymbol{A}$ that have N landmarks, and each landmarks has K points.

$$\boldsymbol{A} = \{A_n \in \boldsymbol{A} \mid 1 \leq n \leq N\}$$
$$A_n = \{{}^nP_1, \cdots, {}^nP_K\} \tag{3.3}$$
$$^nP_k = ({}^nx_k, {}^ny_k, {}^nz_k)$$

Where $\boldsymbol{A}$ is the set of all landmarks, A_n is one of the landmarks, P_k is a point in A_n, $({}^nx_k, {}^ny_k, {}^nz_k)$ is the corresponding coordinates.

We first assume the first landmarks, A_1, is the mean shape, so we apply the approximation process mentioned earlier to match all the other landmarks onto A_1.

$$A_1^T A_2 = U \Sigma V^*, R = V^{*T} U^T, A_2' = A_2 R \qquad (3.4)$$

Where A_2' is the best approximation to A_1 derived from A_2.

After the approximation, we average the coordinates to yield initial mean shape landmarks, M, and apply the same approximation process iteratively until the Frobenius norm of the difference between averaged Markups this round and the previous one is less than 0.0001. Then we get the final mean shape landmarks, M'. Also, we can also know the Procrustes distance of each sample, that is, how far the sample is away from the mean shape in terms of the Frobenius norm.
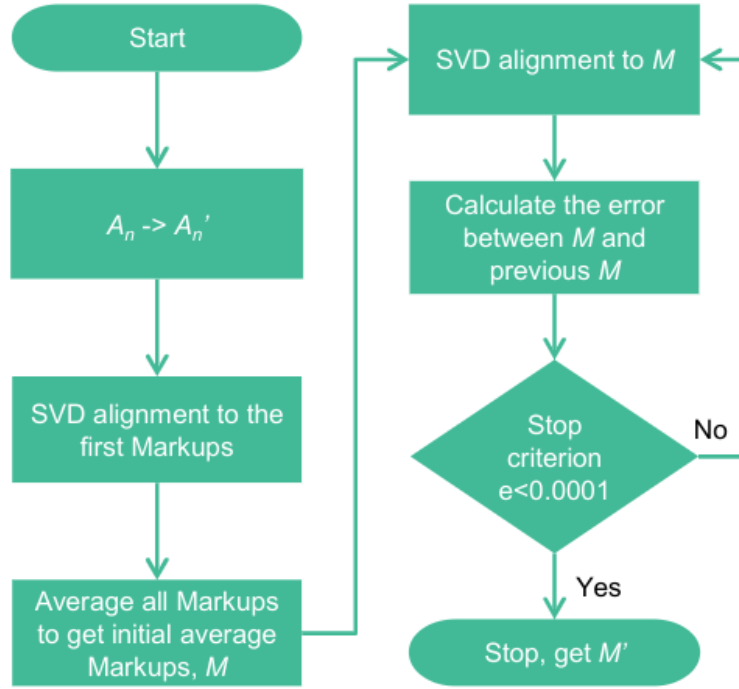

Figure 3.1: GPA flow chart[13]

3.4   Morphospace

A morphospace is a graphical representation of all the morphologies a species or multiple species could have, each point of which represents an individual shape [14]. The axes of morphospace could be any measurement or variables. We construct a 2D morphospace with the first principal component being the x-axis and the second principal component being the y-axis. The morphospace can show the distribution and the clustering of these samples and thus show the relationship in morphology across species.

3.5   Principal Component Analysis

Each point in landmarks provides coordinates data as features. Thus we have N samples with $3K$ features. Conducting PCA on the data can help us find the principal components in shapes. To visualize the morphospace in 3D, we can warp the landmarks on eigenvectors corresponding to a principal component.

$$m = M' + \sum_{i=1}^{t} w_i e_i \qquad (3.5)$$

Where m is the warped landmarks, M' is the mean landmarks, e_i is an eigenvector, w_i is the corresponding weight, m is the morphed landmarks, and t is the number of eigenvectors in use.

Chapter 4   Examples/applications

4.1   Setup

We obtained a total of 9 mesh models (Table 4.1) of Machairodontinae and Felinae

mandibles, downloaded from 3D data sharing website *Morphosource*, courtesy of [9].

Table 4.1
Mandibles mesh models

Subfamily	Taxon	Specimen n°	Age
Machairodontinae	*Pr. ogygia*	B-5264	Late Miocene
	Ma. aphanistus	BAT-1'05 F6-265	Late Miocene
	Am. giganteus	BC-102	Late Miocene
	Me. Sp. Indet.	CB-20	Late Miocene
	X. hodsonae	BC-113	Pleistocene
	H. crenatidens	CB-06	Early Pliocene
Felinae	*Pa. leo*	MNCN COMP-255	Extant
	Pa. uncia	BC-56	Extant
	N. nebulosa	BC-005	Extant

The models are not aligned at first, so we need to place landmarks on the models and then use these landmarks to register these models. The landmarks' position is the same as described in [9], including type I landmarks on anatomical structure and sliding semilandmarks on certain processes (Figure 4.1). We use the orientation matching method mentioned earlier to match the position and orientation. An example is shown in Figure 4.2. After we aligned the landmarks, we applied the same transform to models to register them.
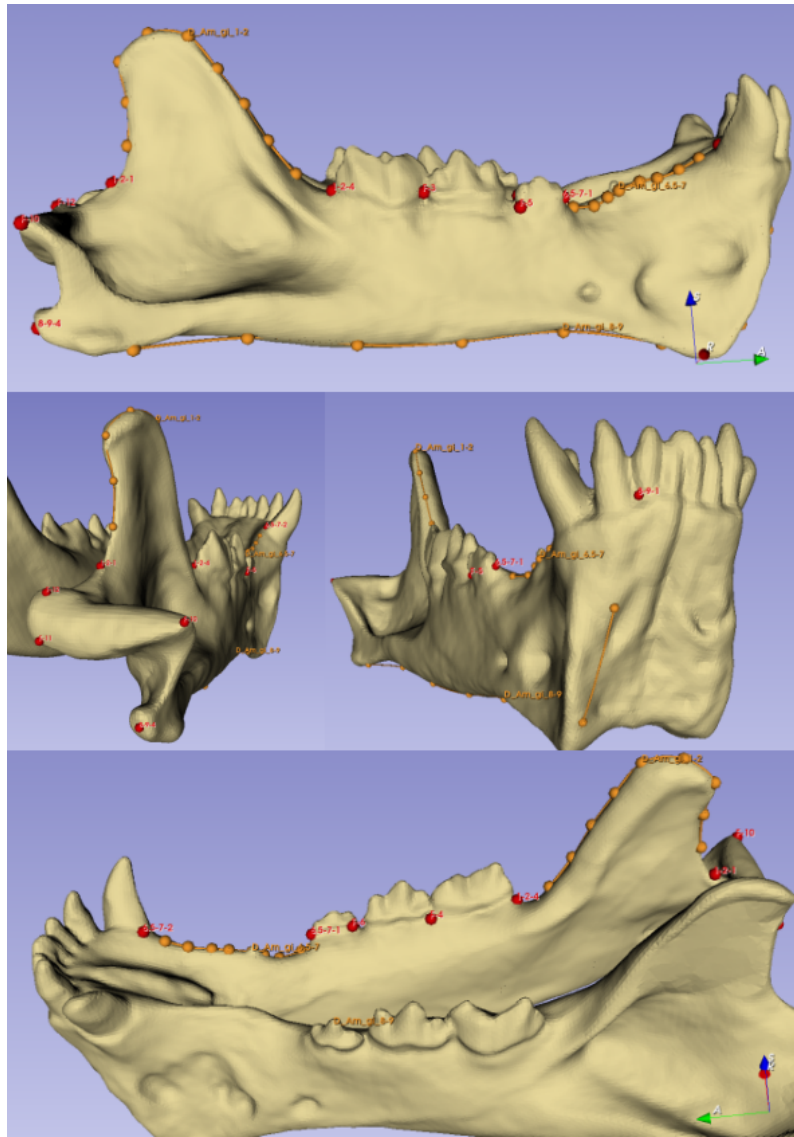

Figure 4.1: landmark point locations, landmark points in red are type I landmarks, while landmark points in orange are semilandmarks.
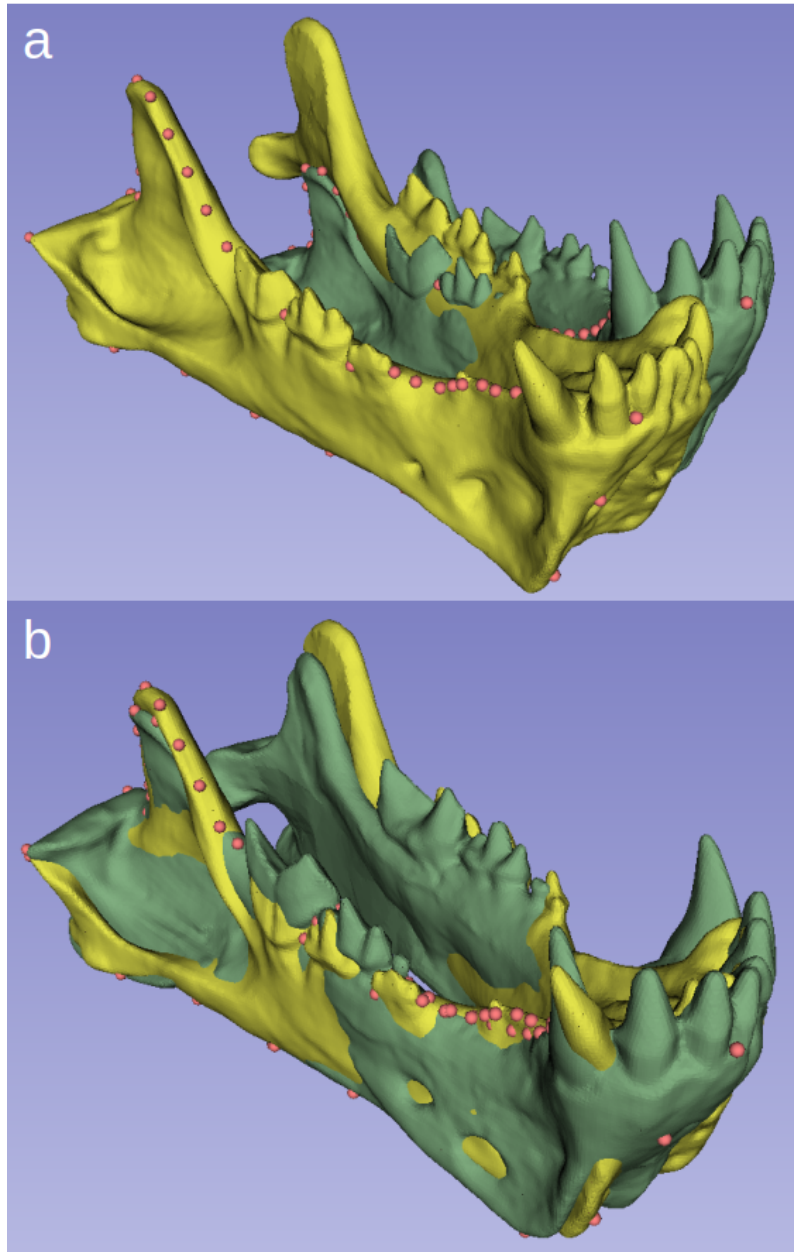
Figure 4.2: registration of landmarks and mesh models. We register the green model onto the yellow model using landmarks. (a) and (b) are the orientation before and after the registration.

4.2 Results

4.2.1 Registration

The registration result of the model is shown in Figure 4.3, and the root mean square error of the landmarks registration is shown in Table 4.2. Notice that *Am. giganteus* being the fixed landmarks so there is no error.
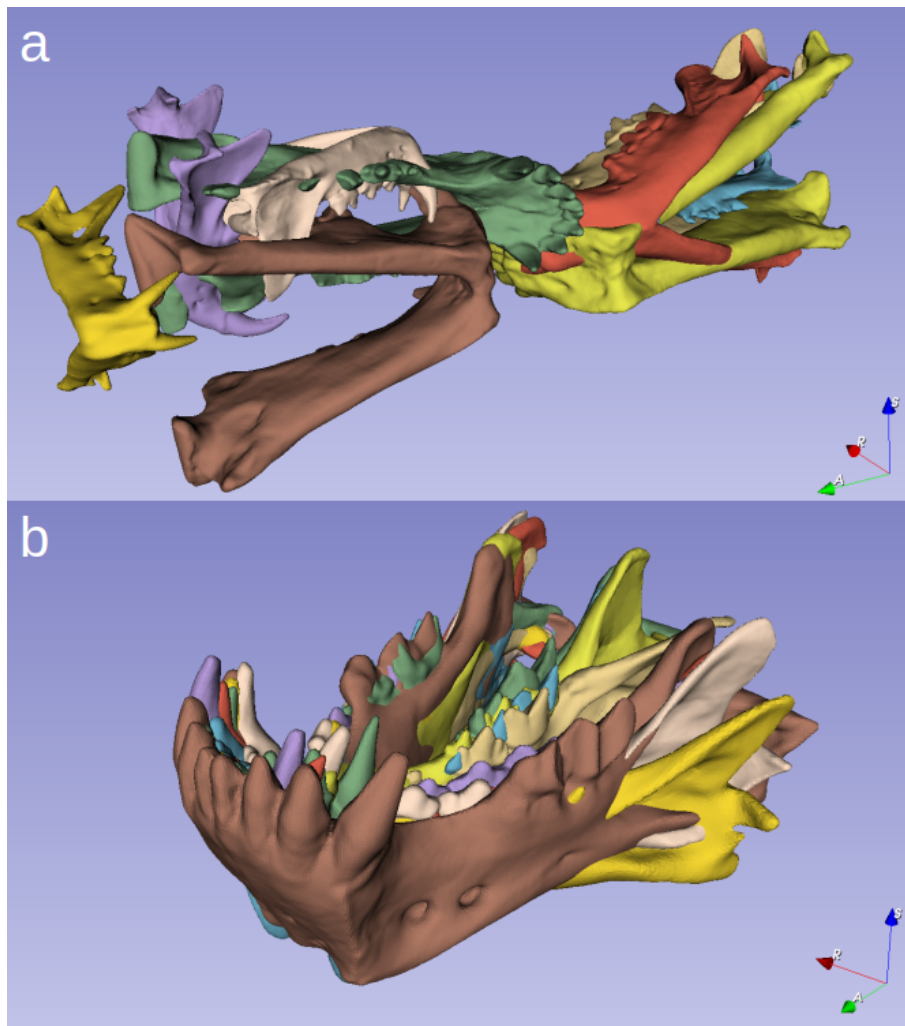

Figure 4.3: (a) is the superimposition of the models before registration, while (b) is the superimposition of models after registration.

4.2.2 GPA

The Procrustes distance (the Frobenius norm a sample is away from the mean) is shown in Table 4.3.

Table 4.2 Registration error		Table 4.3 Procrustes distance	
Sample	RMS Error (unit: mm)	Sample	Procrustes distance
Am. giganteus	X	*Am. giganteus*	0.0620254
H. crenatidens	6.71345	*N. nebulosa*	0.0721631
Ma. aphanistus	10.3556	*Ma. aphanistus*	0.0849159
Me. Sp. Indet.	7.95247	*Pr. ogygia*	0.0853388
N. nebulosa	9.6841	*Pa. leo*	0.0869683
Pa. leo	10.8266	*H. crenatidens*	0.0939499
Pa. uncia	11.5989	*Pa. uncia*	0.0986005
Pr. ogygia	10.8863	*Me. Sp. Indet.*	0.113294
X. hodsonae	10.1941	*X. hodsonae*	0.1377

4.2.3 PCA

The scatter plot on PC1 and PC2 is shown in Figure 4.4. PC1 counts for 68.7% variance, and PC2 counts for 8.9% variance.
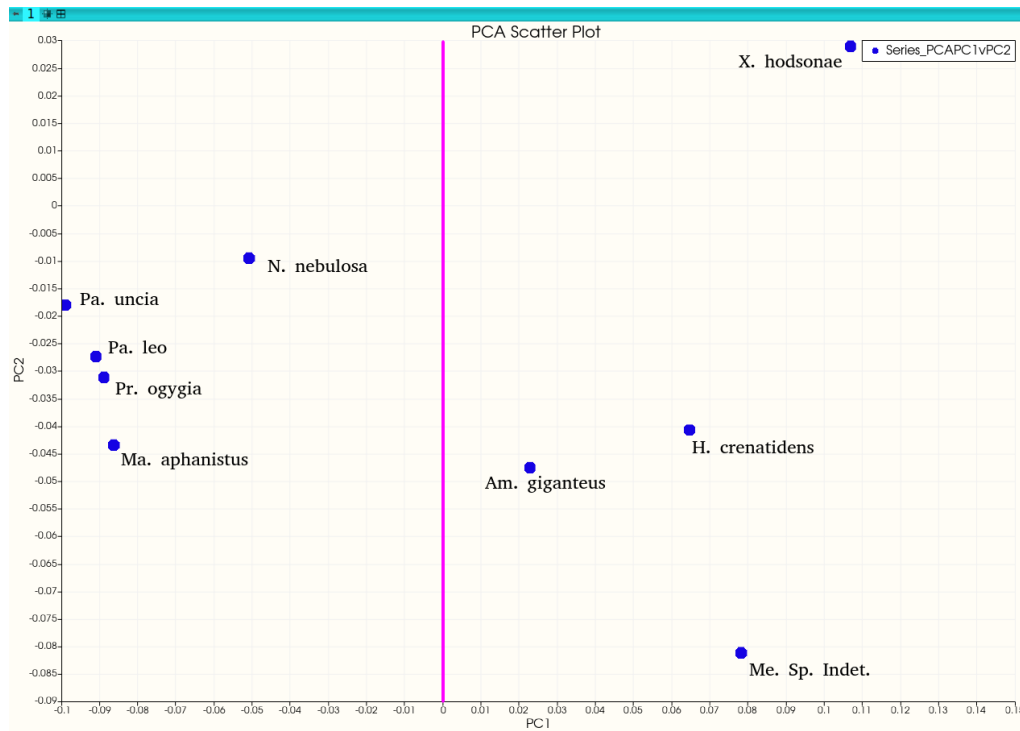

Figure 4.4: result of PCA, successfully separate Felinae and Machairodontinae, while *Pr. ogygia* and *Ma. aphanistus* occupies an intermediate position closer to Felinae.

Chapter 5   Discussion

5.1   Morphospace

From Figure 4.4, we successfully separate Felinae and Machairodontinae. The two target species (*Pr. ogygia* & *Ma. aphanistus*) occupy an intermediate position closer to Felinae. These two target species do not show a large difference in PC1, we have to down to PC2 to separate them better. Thus, they are considered contemporaneous and show no morphological shift. This finding is in favor of the finding in [9]: "*Promegantereon ogygia and Ma. aphanistus clearly overlap along the PC1, but PC2 better separates both taxa, as the latter occupies more positive values, while Pr. ogygia exhibits more negative ones.*" only we have *Pr. ogygia* occupies more positive values in PC2.

5.2   Visualization

We use the lollipop plot vector plot to visualize the morphing direction according to PC1 and PC2 (See Figure 5.1). The morphing direction matches the description in [9]. "*Increasingly positive values on PC1 correspond to a straighter symphyseal region, a straighter ventral plane of the dentary, and a larger mandibular condyle.*" Figure 5.2 shows the warping effect of landmarks and models along PC1.
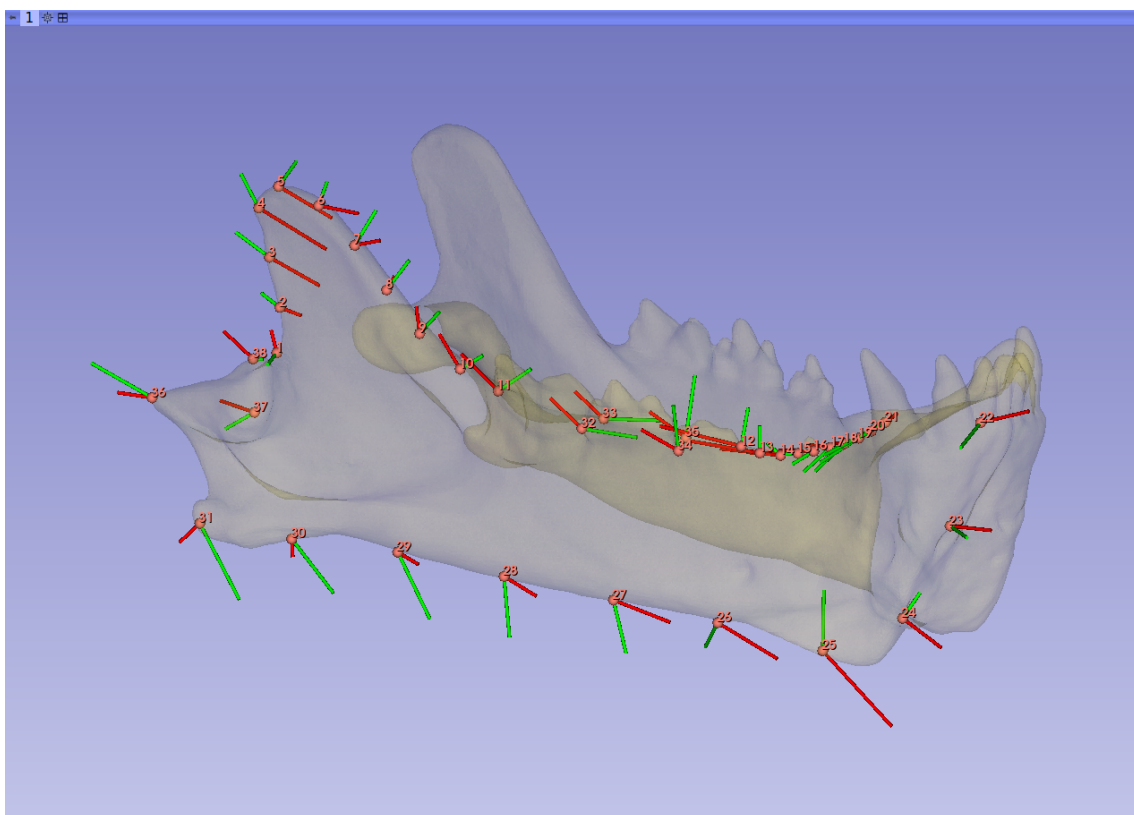
Figure 5.1: Lollipop graph of PC1 and PC2. The vectors in red are for PC1, and the vectors in green are for PC2.
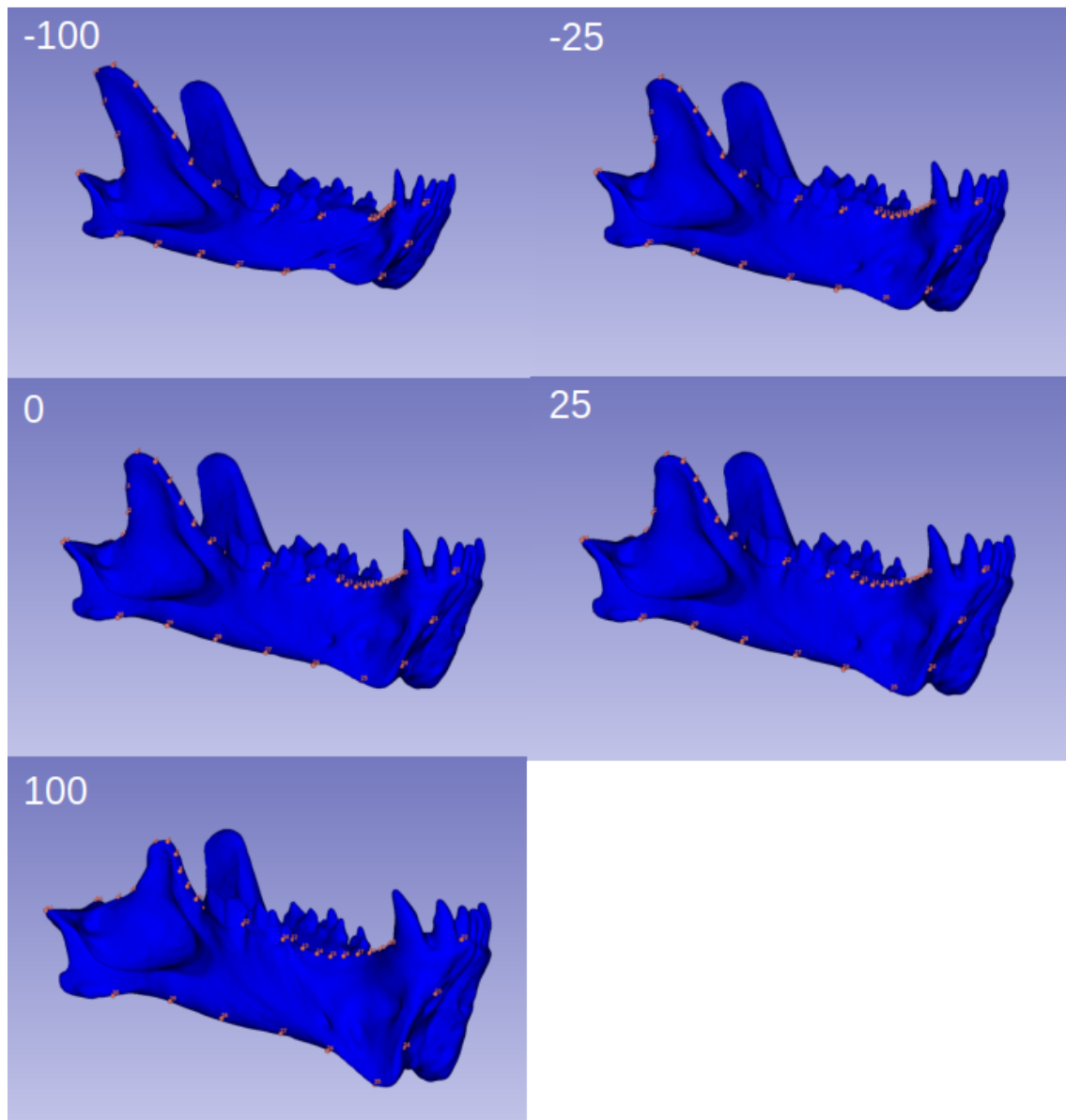
Figure 5.2: morphlogy along PC1. If we increase the value in PC1, the shapes start to have a larger mandibular condyle (the posterior part of the mandible), while decreasing in value results in a smaller condyle.

References

[1] Sara Rolfe, Steve Pieper, Arthur Porto, Kelly Diamond, Julie Winchester, Shan Shan, Henry Kirveslahti, Doug Boyer, Adam Summers, and A Murat Maga. Slicermorph: An open and extensible platform to retrieve, visualize and analyse 3d morphology. Methods in Ecology and Evolution, 12(10):1816–1825, 2021.

[2] Andriy Fedorov, Reinhard Beichel, Jayashree Kalpathy-Cramer, Julien Finet, Jean-Christophe Fillion-Robin, Sonia Pujol, Christian Bauer, Dominique Jennings, Fiona Fennessy, Milan Sonka, et al. 3d slicer as an image computing platform for the quantitative imaging network. Magnetic resonance imaging, 30(9):1323–1341, 2012.

[3] Fedorov. 3d slicer image computing platform. Accessed: 2022-12-28.

[4] Pere M Parés-Casanova. Introductory chapter-morphometric studies: beyond pure anatomical form analysis. New Insights into Morphometry Studies, 2017.

[5] Joan T Richtsmeier, Valerie Burke Deleon, and Subhash R Lele. The promise of geometric morphometrics. American Journal of Physical Anthropology: The Official Publication of the American Association of Physical Anthropologists, 119(S35):63–91, 2002.

[6] Leslie F Marcus. Traditional morphometrics. In Proceedings of the Michigan

morphometrics workshop, volume 2, pages 77–122. The University of Michigan Museum of Zoology Ann Arbor, USA, 1990.

[7] Fred L Bookstein. Morphometric tools for landmark data. Cambridge University Press, 1997.

[8] Gema Siliceo, Manuel J Salesa, Mauricio Antón, Marcos FG Monescillo, and Jorge Morales. Promegantereon ogygia (felidae, machairodontinae, smilodontini) from the vallesian (late miocene, mn 10) of spain: morphological and functional differences in two noncontemporary populations. Journal of Vertebrate Paleontology, 34(2):407–418, 2014.

[9] Narimane Chatar, Valentin Fischer, Gema Siliceo, Mauricio Antón, Jorge Morales, and Manuel J Salesa. Morphometric analysis of the mandible of primitive saber-toothed felids from the late miocene of spain. Journal of Mammalian Evolution, 28(3):753–771, 2021.

[10] Gene H Golub and Charles F Van Loan. Matrix computations. JHU press, 2013.

[11] MonsieurCanuck. Orthogonal procrustes problem — Wikipedia, the free encyclopedia, 2022. [Online; accessed 27-April-2022].

[12] Peter H Schönemann. A generalized solution of the orthogonal procrustes problem. Psychometrika, 31(1):1–10, 1966.

[13] Li-Wei Yang and Ping-Lang Yen. A morphology model for the cyber-physical operation of a remote swabbing robot. International Journal of iRobotics, 5(3):7–12, 2022.

[14] Simplificationalizer. Morphospace — Wiktionary, the free dictionary, 2022. [On-line; accessed 17-March-2022].